

Structure Evolution in High- T_c Bi-Based Superconductors with Pb Doping Revealed by Electron Microscopy

XIAO-JING WU* AND SHIGEO HORIUCHI†

National Institute for Research in Inorganic Materials, Tsukuba, Ibaraki, 305, Japan

AND LINA BEN-DOR AND HUSSAM DIAB

Department of Inorganic and Analytical Chemistry, Hebrew University, Jerusalem 91904, Israel

Received June 3, 1991; in revised form September 6, 1991

The structural evolution of a series of Pb-doped Bi-based superconductors, composed mainly of the high- T_c phase, has been studied by transmission, as well as scanning, electron microscopy. It has been observed in all specimens that a minor (2212) phase is often intergrown within a (2223) phase matrix and that impurity phases also coexist. In the specimen annealed for 56 hr at 870°C the (2223) phase contains a Bi-type structural modulation, with $\mathbf{q} = \mathbf{b}^*/4.93$. In the specimen annealed for 90 hr, besides the Bi-type modulation with $\mathbf{q}_1 = \mathbf{b}^*/4.95$, a Pb-type modulation with $\mathbf{q}_2 = \mathbf{b}^*/7.71$ has been observed frequently. In some regions adjoining grains are in a twin relationship around [001], but often the rotation angle is not exactly 90°; i.e., the [100] of one grain is deviated slightly from the [010] of another grain. In the specimen annealed for 95 hr the Bi-type modulation has $\mathbf{q}_1 = \mathbf{b}^*/5.00$, whereas the satellites caused by the Pb-type modulation become too diffuse to determine \mathbf{q}_2 . In some local areas the twin planes are not parallel to (001). In some grain boundaries along (001), thin amorphous regions, rich in Ca, are often formed. The relationship between microstructure and superconductivity is discussed.

© 1992 Academic Press, Inc.

1. Introduction

It is known that in the Bi-based superconductor system there are three major superconducting phases, with compositions $\text{Bi}_2\text{Sr}_2\text{Ca}_{n-1}\text{Cu}_n\text{O}_x$ ($n = 1, 2, 3$), viz. the (2201), (2212), and (2223) phases, respectively (1). Since the (2223) phase has the

highest T_c , is more stable in air than Y-based superconductors, and has a much lower toxicity than Tl-based superconductors, it is necessary, from the viewpoint of practical use, to prepare single phase (2223). For this purpose many methods have been tested, such as partial substitution of bismuth by lead (2-6) or antimony (7) and doping by fluorine (8-10).

Recently, Ben-Dor *et al.* (11) reported the synthesis of Pb-doped bulk samples by the sol-gel method. Samples of $\text{Bi}_{1.8}\text{Pb}_{0.2}\text{Sr}_2\text{Ca}_2\text{Cu}_3\text{O}_x$ were annealed for 56, 90, and 95

* Present address: Corporate Research Laboratory, Mitsubishi Gas Chemical Co., Inc., Wadai 22, Tsukuba, Ibaraki, 305, Japan.

† To whom correspondence should be addressed.

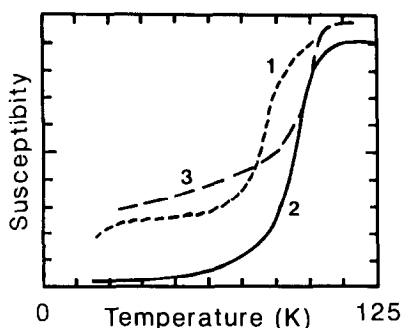


FIG. 1. Magnetic susceptibility vs temperature for $\text{Bi}_{1.8}\text{Pb}_{0.2}\text{Sr}_2\text{Ca}_2\text{Cu}_3\text{O}_x$ annealed at 870°C (line 1) for 56 hr, (line 2) for 90 hr, and (line 3) for 95 hr (from Ref. (11)).

hr in air at 870°C and will be called samples 1, 2, and 3, respectively, in the present paper. Magnetic susceptibility vs temperature curves showed evident differences between the samples (Fig. 1). According to X-ray diffraction analysis, it was estimated that the volume ratio of the (2223) phase (pseudo-tetragonal, $a \approx b = 0.54$ and $c = 3.70$ nm) to the (2212) phase (pseudo-tetragonal, $a \approx b = 0.54$ and $c = 3.08$ nm) is about 3 : 1 in sample 1 and 12 : 1 in sample 2. Furthermore, magnetic measurements showed marked differences between samples 2 and 3, but X-ray diffraction patterns did not reveal any clear differences between them; i.e., the ratio of (2223) to (2212) is almost the same in these two samples. Since the superconducting characteristics in high- T_c superconductors strongly depend on the local structures, it is important to examine these samples from the viewpoint of microstructure analysis.

In the present paper transmission electron microscopes (TEM) and a scanning electron microscope (SEM) equipped with an energy dispersive X-ray spectrometer (EDX) have been employed to examine the microstructure, as well as the local compositions, of these three samples. The influence of microstructure on the superconductivity of the samples will also be discussed.

2. Experimental

The samples with nominal composition $\text{Bi}_{1.8}\text{Pb}_{0.2}\text{Sr}_2\text{Ca}_2\text{Cu}_3\text{O}_x$ have been prepared as reported in Ref. (11). The sintered samples were fractured, the exposed planes were polished mechanically, and the polished surfaces were examined by SEM.

In order to observe the interface between grains by TEM, thin specimens were prepared by an ion-milling method; the bulk samples were polished mechanically down to about $40 \mu\text{m}$ in thickness. A Gatan 600N-DP ion-milling machine equipped with a liquid nitrogen stage was used to mill the specimens under the following conditions; accelerating voltage of 4.5 kV, Ar-ion current of 1.0 mA, and incident angle of 14° .

An Akashi DS130 SEM equipped with an EDX (Philips 9900), a JEM-2000EX TEM operated at an accelerating voltage of 200 kV, and a Hitachi FE-2000 TEM equipped with a field emission gun and EDX were additionally used to analyze the composition of local areas.

3. Results

Figure 2 shows several SEM micrographs. In Fig. 2a, taken from sample 1, EDX analysis identified the needle-like regions, as well as regions with gray contrast, as corresponding to superconducting phases, while regions with dark contrast correspond to impurity phases such as $(\text{Sr,Ca})_3\text{Cu}_5\text{O}_y$ and $(\text{Sr,Ca})_2\text{CuO}_x$. These phases have been found extensively in Bi-based superconductors without Pb (12–14). The needles are probably the cross section of plate-like superconducting grains. In Fig. 2b, taken from sample 2, the needle-like regions disappear and the gray contrast regions consisting of a superconducting phase seem more uniform than those observed in Fig. 2a. Figure 2c, taken from sample 3, seems somewhat similar to Fig. 2b but an

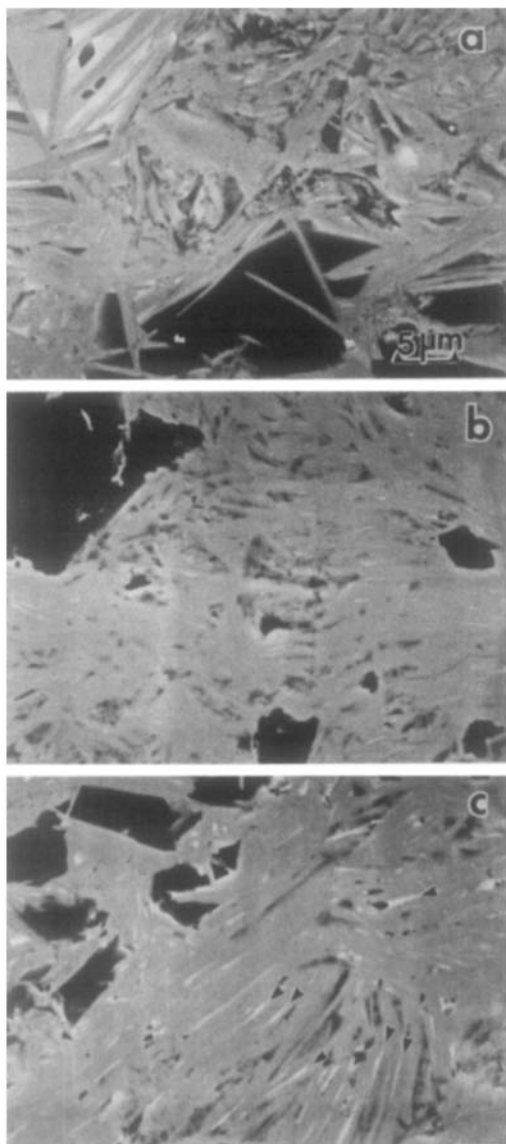


FIG. 2. SEM micrographs (a), (b), and (c) from samples 1, 2, and 3, respectively. The regions with white contrast indicated by arrowheads in (c) correspond to a Ca-rich impurity phase.

obvious difference is that some white contrast regions, indicated by small arrowheads, occur frequently. These white contrast regions are too small to analyze the chemical composition quantitatively by

EDX; a qualitative analysis, however, indicates that these regions are rich in Ca.

Furthermore, TEM observations give additional information about the microstructures of these specimens. Figures 3a and 3b show two electron diffraction patterns taken from sample 1 with the incident beam along the [100] direction. All the main spots in (a) can be identified with the (2223) phase. It should be noted that for Fig. 3b a minor (2212) phase is mixed with the major (2223) phase. Although X-ray diffraction analysis showed that the ratio of (2223):(2212) phases is 3 : 1, an isolated grain of the (2212) phase was never found in this specimen; the minor (2212) phase occurs intergrown within the (2223) matrix.

Figure 4 shows a lattice image of a grain boundary taken along [110]. The (001) planes of two grains are tilted by about 10° . The matrix consists of the (2223) phase for both grains, while the (2212) phase is intergrown within the matrix in a small area, marked by two pairs of horizontal arrowheads. The vertical arrows indicate the stacking faults.

Figures 5a and 5b show two EDPs taken from sample 2 along [100] and [010], respectively. From Fig. 5a it is found that there are two modulation waves: one modulation corresponds to the average wave vector $\mathbf{q}_1 = \mathbf{b}^*/4.95$, while the other to $\mathbf{q}_2 = \mathbf{b}^*/7.71$. It is known that the former (m_1) is related to the displacement of Bi atoms from their average positions along the b and c axes (15–18), which is caused by the insertion of extra oxygen atoms. The latter (m_2) is believed due to the addition of Pb (19, 20), because it has never been found in the absence of Pb. Zandbergen *et al.* (21) have classified the modulations m_1 and m_2 as Bi-type and Pb-type, respectively. The former relates to the positional modulation of Bi atoms, while the latter to that of Pb atoms. In Fig. 5b the coexistence of (2223) and (2212) can be seen. It is again identified by TEM observations that the (2212) phase al-

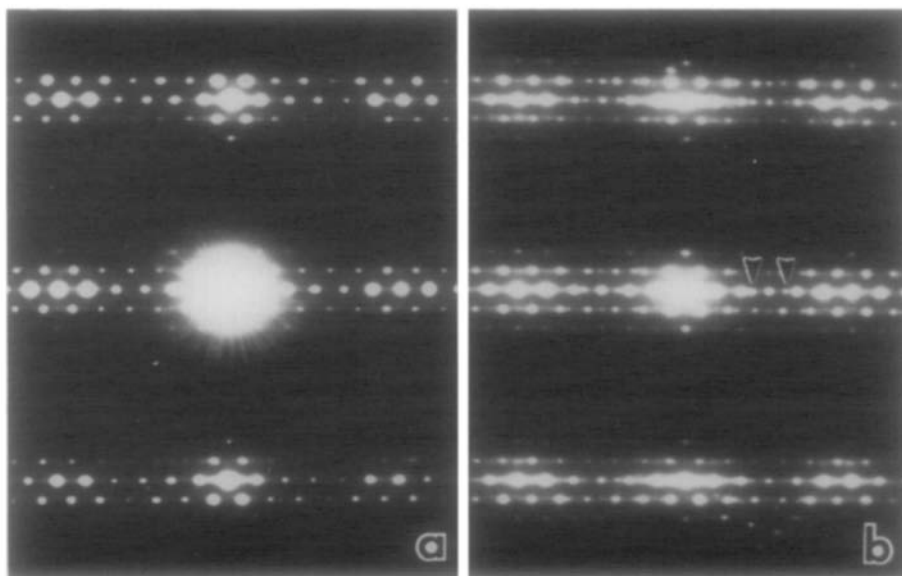


FIG. 3. EDPs from sample 1 taken with the incident electron beam along [100]. In (a) all diffraction spots can be indexed based on the (2223) phase. (b) shows the intergrowth of the minor (2212) phase within the major (2223) matrix. The spots from (2212) are indicated by arrowheads.

ways exists in this specimen as stacking faults.

Figure 6 shows the boundary area between grains A and B in sample 2. In a low magnification image, Fig. 6a, a horizontal arrowhead indicates the boundary and some stacking faults occur near it. The vertical arrowheads in grain B indicate some dark bands normal to the (001) planes. The spacing between adjacent bands is not constant, but change in the range from 35 to 60 nm. A possible origin for these bands is the nonuniform distribution of Bi and Pb atoms. In an enlarged image, Fig. 6b, small vertical arrowheads indicate the fringes from Pb-type modulation, while a pair of medium-sized arrowheads show the intergrowth of (2212) within the (2223) matrix.

For grain A in Fig. 6, it is known from its EDP that the [010] direction is exactly along the incident electron beam. For grain B, on the other hand, the [100] direction deviates from the incident beam by several degrees,

although the (001) plane is parallel to that of grain A. This is the reason why the contrast for A and B is different. In other words, there is not an exact 90° twin relationship between grains A and B. This is a little different from what has been found in many Bi-based superconductors (for example, (21–23)), and this implies that the coherence of the lattice planes between A and B is not good; i.e., the connection between them is probably weak. Similar cases have frequently been observed in sample 2, although the deviation angle between [100] and [010] is not constant. Noncoherent boundaries between grains have been reported by Ramesh *et al.* in a Bi-based superconductor without Pb (24).

Figure 7a is a high resolution image of sample 3. The arrowhead pointing to the right indicates a region with a dislocation, while the arrow pointing to the left indicates a (001) 90° twin boundary. An unusual orientation change occurs; in region A the inci-

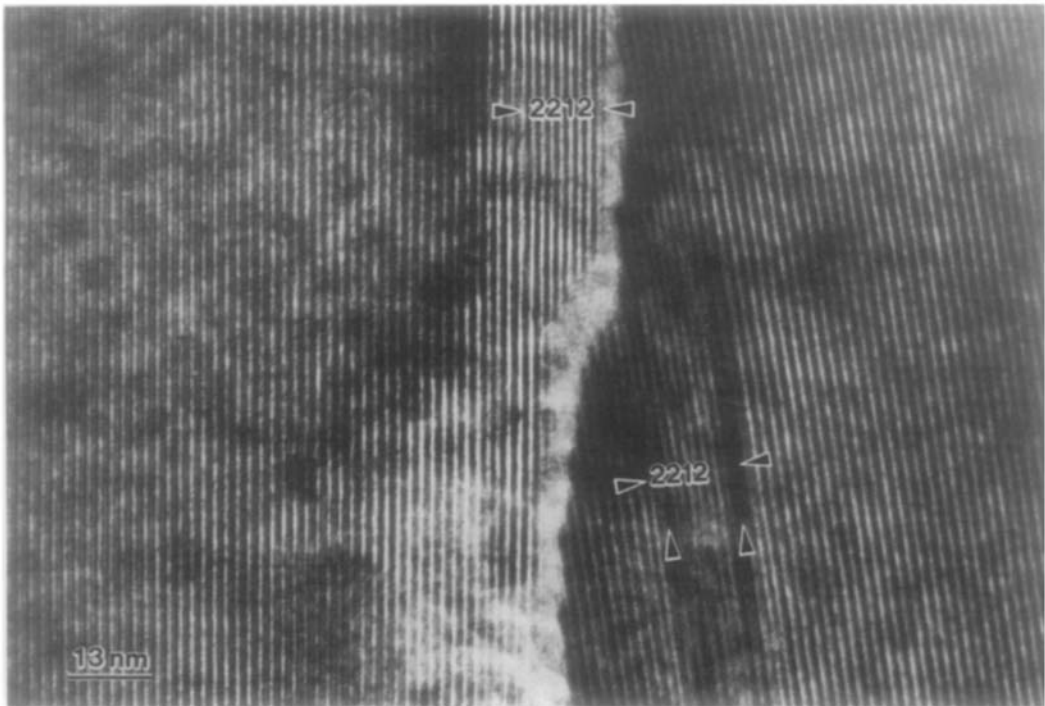


FIG. 4. A lattice image of a grain boundary from sample 1 taken with the incident electron beam along $[110]$. The angle between the (001) planes of the two grains is about 10° . Two pairs of horizontal arrowheads indicate the $(22)2$ regions, while the vertical arrowheads show the presence of stacking faults.

dent beam is along the $[100]$ zone, while in region B it is along $[010]$. Between A and B there is a transition region T, in which no clear boundary is seen. The (001) planes seem to extend continuously from A to B. Figure 7b shows schematically the change in the direction of the modulation at the twin boundary, which is not parallel to (001) but to the small step facets. As a result, the orientation changes from area A to B within transition region T, as shown in the projection image.

Figure 8 is another image taken from sample 3. Among the grain boundaries a nonsuperconducting amorphous phase is present. The width of the amorphous area is about 10 nm. In the left part of the photograph the interchange between the $[010]$ and $[100]$ axes is again seen. It should be emphasized

that neither such an amorphous area between grain boundaries nor a change in the direction of modulation has been observed in sample 2.

A TEM equipped with EDX was used to identify the composition of the amorphous regions qualitatively. The results show that the amorphous phase contains more Ca than the superconducting phase. It is obvious, from the viewpoint of composition analysis as well as image contrast, that these regions are not formed by damage during ion-milling.

4. Discussion

4.1. Structural Characteristics

Table I summarizes the results of electron diffraction analysis for the modulation

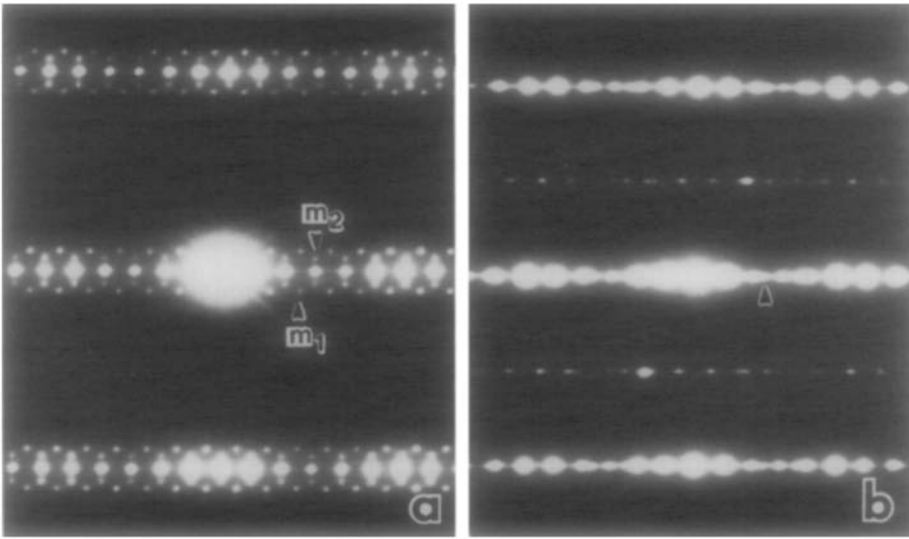


FIG. 5. EDPs from sample 2 taken with the incident beam along [100] (a) and along [010] (b). There are two types of modulation waves, m_1 and m_2 , in the sample. The spot labeled by an arrowhead in (b) indicates an intergrown (2212) phase.

structures in these specimens. The wave vectors for the Bi-type modulations are almost the same for samples 1 and 2, and decrease slightly for sample 3. It was proposed by Zandbergen *et al.* (17) that the Bi-type modulation is produced by the presence of extra oxygen atoms in the Bi-O layers. A change in the oxygen content must then lead to a change in the modulation period; an increase in oxygen atoms should decrease the Bi-type modulation period, while a decrease in the amount of oxygen should increase the modulation period. Hence, if this model is correct, the increase of the average modulation period of sample 3 implies indirectly that its average oxygen content is less than that found in samples 1 and 2.

It has been reported that the Bi- and Pb-type modulations are coherent, since some extra spots corresponding to $m(\mathbf{q}_1 - \mathbf{q}_2)$ (m , integer) are observed in EDPs (21, 25). In samples 2 and 3, however, no such spots are observed. But some proof can also be found

to certify that these two modulations are not entirely independent. From Table I it is observed that when there is no Pb-type modulation, as in sample 1, third-order satellites appear (Fig. 3). This means that the displacement modulation wave of Bi is not a sinusoidal wave (21). However, when the Pb-type and Bi-type modulation occur simultaneously, as in sample 2, only first-order satellites appear (Fig. 5), and hence the displacement modulation wave of Bi must be very near to a sinusoidal wave. In sample 3, on the other hand, the Pb-type modulation is not perfect. Because the second-order satellites of Bi-type modulation are observed, the modulation state of sample 3 is between that observed in samples 1 and 2. From these results it can be concluded that these two types of modulations are not independent; i.e., the occurrence of the Pb-type modulation evidently affects the Bi-type modulation. The Pb-type modulation seems more sensitive to annealing than the Bi-type modulation.

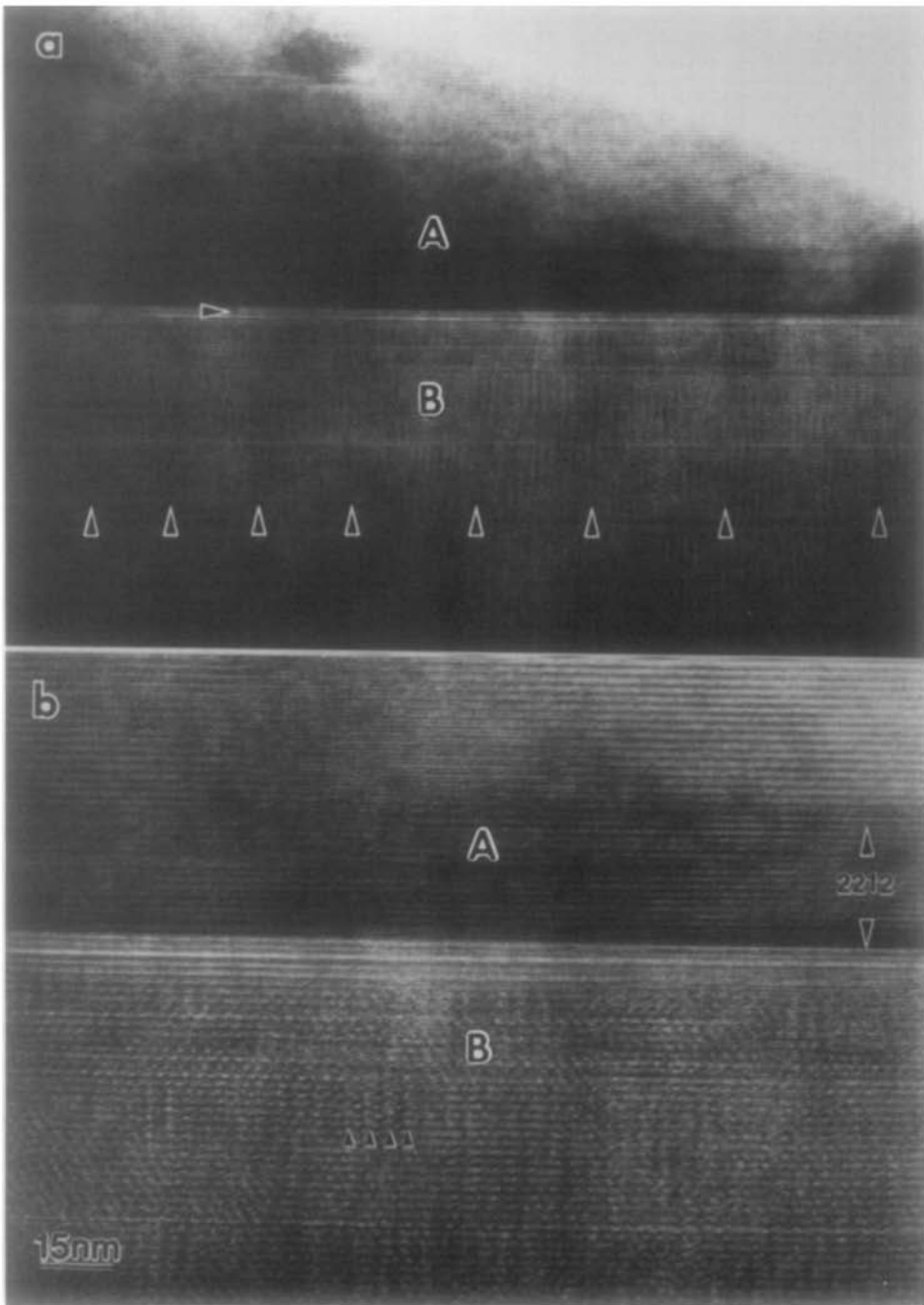


FIG. 6. (a) A boundary area between grains A and B in sample 2. (b) Enlarged image of (a), in which vertical small arrowheads show the fringes from Pb-type modulation.

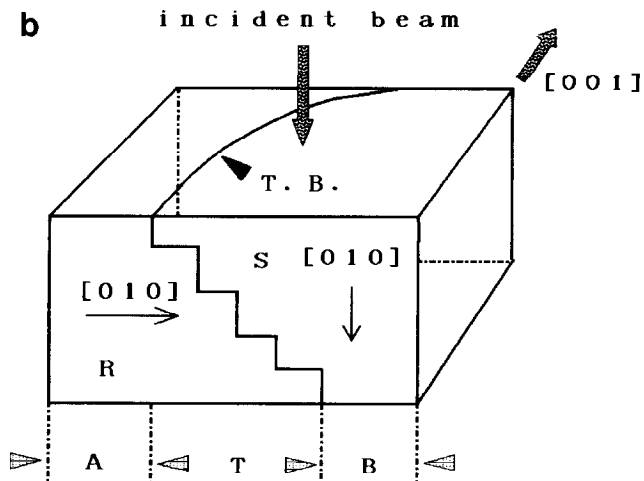
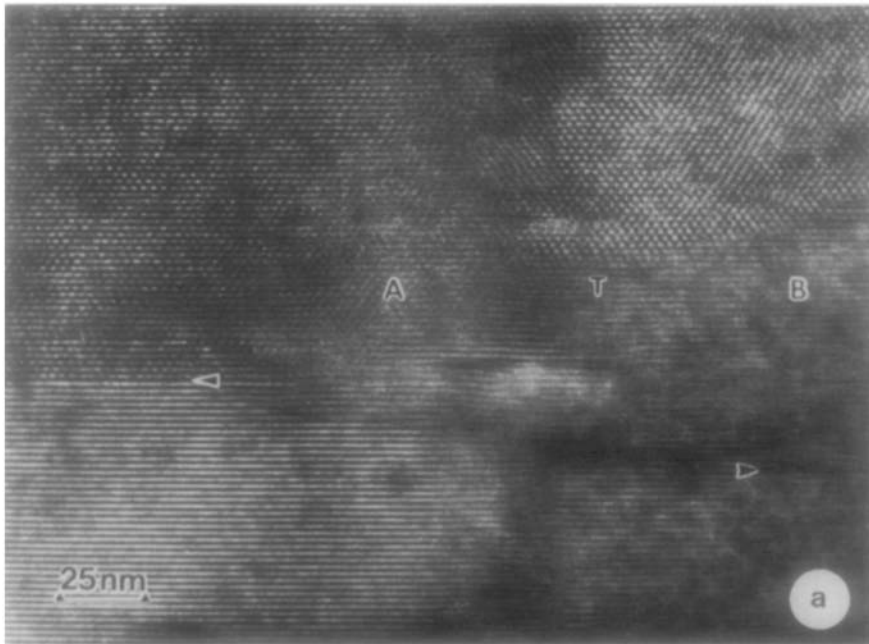


FIG. 7. (a) A high resolution image of sample 3. The arrowhead pointing to the right indicates a dislocation, and the arrowhead pointing to the left indicates a twin boundary of 90° rotation. Between regions A and B the direction of modulation changes by 90° around [001]. (b) A schematic diagram showing the change of modulation direction observed in Fig. 7a. The direction of modulation is horizontal in region R and vertical in region S. Region A is from the projection of R, region B is from the projection of S, and region T is from the overlapped projection of R and S. T.B. means a twin boundary.

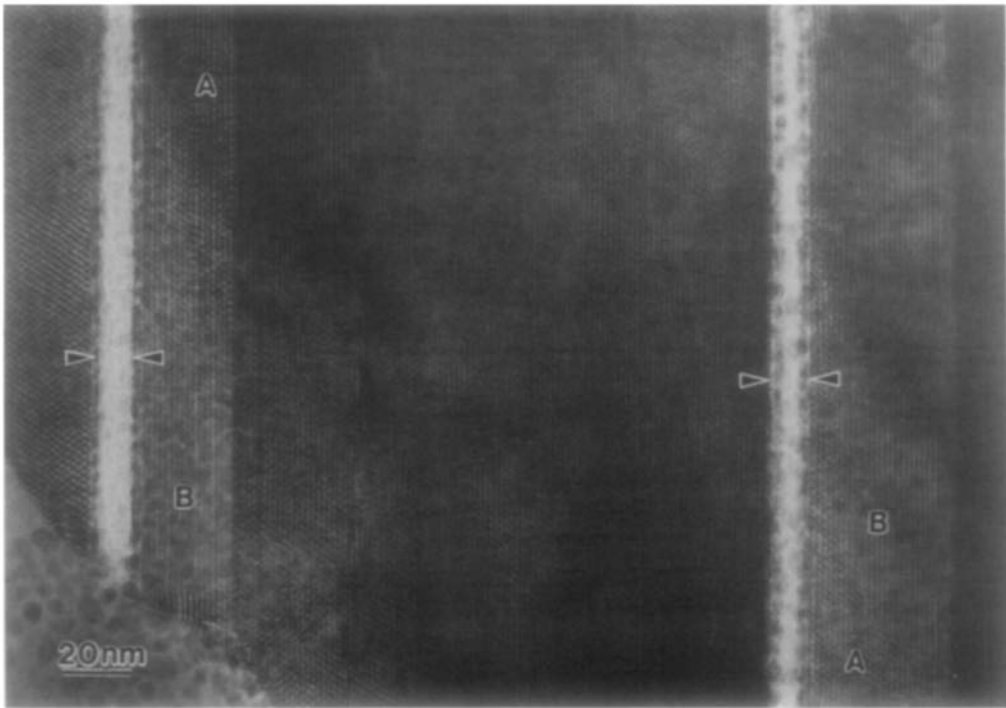


FIG. 8. A lattice image showing grain boundaries in sample 3. An amorphous phase often appears at the boundaries with a width of about 10 nm. The modulation direction changes by 90° between regions A and B.

In a SEM photograph, Fig. 2c, a number of regions with white contrast are observed. It is recognized from the EDX analysis that these regions are Ca rich. TEM observation in Fig. 8 shows that an amorphous phase is

formed at the boundary between two superconducting grains and, according to the EDX analysis, this is also a Ca-rich phase. It may be concluded that the white contrast regions in Fig. 2c are identical to the amorphous regions in the grain boundary in Fig. 8.

The structural evolution of the samples as a function of annealing period can be briefly outlined. In the specimen annealed for 56 hr, the (2223) phase was formed as the main phase. Since only a Bi-type modulation occurs, the distribution of Pb atoms must be random in the Bi(Pb)-O planes. When the annealing period is increased to 90 hr, the distribution of Pb atoms in the (2223) phase becomes ordered in most of the grains, and the minor (2212) phase is reduced in volume. In the sample further annealed (95 hr), the change in the distribution of Pb atoms be-

TABLE I

WAVELENGTHS OF BI- AND Pb-TYPE MODULATIONS (λ_1 AND λ_2) IN THE b DIRECTION AND THE MAXIMUM ORDER OF SATELLITES VISIBLE IN THE DIFFRACTION PATTERNS (N) FOR SAMPLES HEATED FOR 56, 90, AND 95 HR AT 870°C

Sample	λ_1	λ_2	N
1	4.93	—	3
2	4.95	7.71	1
3	5.00	^a	2

^a It could not be determined because the satellites are diffuse.

comes slightly irregular and, from the viewpoint of modulation wavelength, the average oxygen content must have decreased slightly in the grains. In addition, an amorphous phase develops at the grain boundaries. Since the Bi-type modulation is not independent of the Pb-type modulation, the degradation of the Pb-type modulation must have caused not only the rearrangement of Pb atoms but also the Bi atoms. This can be related to the observation that in local areas the Bi-type modulation has changed the direction by 90° on a Bi(Pb)–O plane (see Figs. 7a and 8).

4.2. Microstructure and Superconducting Properties

Different annealing periods produced large differences in the superconducting properties for the $\text{Bi}_{1.8}\text{Pb}_{0.2}\text{Sr}_2\text{Ca}_2\text{Cu}_3\text{O}_x$ samples, as shown in Fig. 1. X-ray diffraction patterns (11) showed that sample 1 contains more low- T_c (2212) phase than sample 2. Hence, it can be understood why there is a significant difference in the magnetic susceptibility between these two samples.

For sample 3 a marked change was found in the magnetic susceptibility, while X-ray diffraction showed no clear change from that of sample 2. Based on the microstructure analysis the reasons for this difference can be interpreted as follows: first, both TEM and SEM observations reveal the existence of an amorphous phase in sample 3. Since the amorphous phase is nonsuperconducting, its occurrence decreases the magnetic susceptibility of the specimen. Second, electron diffraction analysis showed that for sample 3 the Bi-type modulation period increased slightly, suggesting that the oxygen content decreased. It has been reported by Bokhimi *et al.* (26) that for the (2223) phase T_c decreased when the oxygen deficiency was increased. If the oxygen deficiency is not uniform, but changes from grain to grain, T_c should vary among grains. The grains with different T_c will produce a

slow drop in the susceptibility curve, as seen in Fig. 1.

Acknowledgments

The authors thank S. Isakozawa and T. Kamino of Hitachi Ltd. for their help with EDX analysis by TEM (FE-2000), M. Tsutsumi of NIRIM for his help in SEM observations, Y. Kitami and M. Yokoyama for the TEM maintenance, and Dr. S. Markgraf for English corrections. One of the authors (Wu) would like to express his sincere appreciation to the Science and Technology Agency, Japan, for offering the fellowship. The financial support of the Ministry of Science and Technology, Israel, is gratefully acknowledged by the Israeli group (Ben-Dor, Diab).

References

1. H. MAEDA, Y. TANAKA, M. FUKUTUMI, AND T. ASANO, *Jpn. J. Appl. Phys.* **27**, L209 (1988).
2. M. TAKANO, J. TAKADA, K. ODA, H. KITAGUCHI, Y. MIURA, Y. IKEDA, Y. TOMII, AND H. MAZAKI, *Jpn. J. Appl. Phys.* **27**, L1041 (1988).
3. S. A. SUNSHINE, T. SIEGRIST, L. F. SCHNEEMEYER, D. W. MURPHY, R. J. CAVA, B. BATLOGG, R. B. VAN DOVER, J. V. WASZCZAK, J. H. MARSHALL, P. MARSH, L. W. RUPP, JR., AND W. F. PECK, *Phys. Rev. B* **38**, 893 (1988).
4. U. ENDO, S. KOYAMA, AND T. KAWAI, *Jpn. J. Appl. Phys.* **27**, L1476 (1988).
5. R. J. CAVA, B. BATLOGG, S. A. SUNSHINE, T. SIEGRIST, R. M. FLEMING, K. RALEE, L. F. SCHNEEMEYER, D. W. MURPHY, R. B. VAN DOVER, P. K. GALLAGHER, S. H. GLARUM, S. NAKAHARA, R. C. FARROW, J. J. KRAJEWSKI, S. M. ZAHURAK, J. V. WASZCZAK, J. H. MARSHALL, P. MARSH, L. W. RUPP, JR., W. F. PECK, AND E. A. RIETMAN, *Physica C* **153–155**, 560 (1988).
6. B. W. STATT, Z. WANG, M. J. G. LEE, J. V. YAKHMI, P. C. DE CAMERGO, J. F. MAJOR, AND J. W. RUTTER, *Physica C* **156**, 251 (1988).
7. H. LIU, X. ZHAN, Y. CHAO, G. ZHOU, Y. RUAN, Z. CHEN, AND Y. ZHANG, *Physica C* **156**, 804 (1988).
8. S. HORIUCHI, K. SHODA, H. NOZAKI, Y. ONODA, AND Y. MATSUI, *Jpn. J. Appl. Phys.* **28**, L621 (1989).
9. S. HORIUCHI, K. SHODA, AND Y. MATSUI, *J. Ceram. Soc. Jpn. Int. Ed.* **97**, 977 (1989).
10. X. GAO, X. WU, H. YAN, Z. YIN, C. LIN, Y. FU, AND W. XIE, *Mod. Phys. Lett. B* **4**, 137 (1990).
11. L. BEN-DOR, H. DIAB, AND I. FELNER, *J. Solid State Chem.* **88**, 183 (1990).
12. S. IKEDA, H. ICHINOSE, T. KIMURA, T. MATSU-

- MOTO, H. MAEDA, Y. ISHIDA, AND K. OGAWA, *Jpn. J. Appl. Phys.* **27**, L999 (1988).
13. S. HORIUCHI, K. SHODA, X. J. WU, H. NOZAKI, AND M. TSUTSUMI, *Physica C* **168**, 205 (1990).
 14. R. S. ROTH, C. J. RAWN, J. J. RITTER, AND B. P. BURTON, *J. Am. Ceram. Soc.* **72**, 1545 (1989).
 15. Y. MATSUI, H. MAEDA, Y. TANAKA, AND S. HORIUCHI, *Jpn. J. Appl. Phys.* **27**, 372 (1988).
 16. S. HORIUCHI, H. MAEDA, Y. TANAKA, AND Y. MATSUI, *Jpn. J. Appl. Phys.* **27**, L1172 (1988).
 17. H. W. ZANDBERGEN, W. A. GROEN, F. C. MIJLHOFF, G. VAN TENDELOO, AND S. AMELINCKX, *Physica C* **156**, 325 (1988).
 18. Y. LE PAGE, W. R. MCKINNON, J.-M. TARASCON, AND P. BARBOUX, *Phys. Rev. B* **40**, 6810 (1989).
 19. S. IKEDA, K. AOTA, T. HATANO, AND K. OGAWA, *Jpn. J. Appl. Phys.* **27**, L2040 (1988).
 20. R. RAMESH, G. VAN TENDELOO, G. THOMAS, S. M. GREEN, AND H. L. LAO, *Appl. Phys. Lett.* **53**, 2220 (1988).
 21. H. W. ZANDBERGEN, W. A. GROEN, A. SMIT, AND G. VAN TENDELOO, *Physica C* **168**, 426 (1990).
 22. Y. MATSUI, H. MAEDA, Y. TANAKA, E. TAKAYAMA-MUROMACHI, S. TAKEKAWA, AND S. HORIUCHI, *Jpn. J. Appl. Phys.* **27**, L827 (1988).
 23. O. EIBL, *Physica C* **168**, 239 (1990).
 24. R. RAMESH, B. G. BAGLEY, J. M. TARASCON, S. M. GREEN, M. L. RUDEE, AND H. L. LUO, *J. Appl. Phys.* **67**, 379 (1990).
 25. J. G. WEN, C. Y. YANG, Y. F. YAN, AND K. K. FUNG, *Phys. Rev. B* **42**, 4117 (1990).
 26. A. BOKHIMI, L. GARCIA-RUIZ, E. OROZCO, R. ASOMOZA, AND M. ASOMOZA, *Physica C* **159**, 654 (1989).